Lecture 8 – Quantum Trajectories II

We have suggested that the operator master equation for a photoemissive source is statistically equivalent to a stochastic quantum mapping. Each iteration of the mapping involves a quantum evolution under a nonunitary Schrödinger equation, for a random interval of time, followed by a wavefunction collapse at the end of this interval. In general, the probability distribution governing the duration of the quantum evolution depends on the past history of the source. In most cases it will be very difficult to implement this mapping analytically. However, it is quite easy to implement on a computer. The computer simulations generate "trajectories" for a stochastic wavefunction that describes the current state of the quantum-mechanical source, conditioned on a particular past history of coherent evolution and collapse. Time series obtained from these trajectories have a direct statistical correspondence to the fluctuating signals obtained by monitoring a single quantum system (not an ensemble) in the laboratory. They can be analyzed like experimental data – for a stationary process, by averaging in time; the time averages reproduce the usual quantum-mechanical average.

We now apply this quantum trajectory method to various elementary examples, and show that it reproduces results obtained by conventional methods. The material presented in this lecture is taken from a presentation by Carmichael and Tian at the 1990 Annual Meeting of the Optical Society of America [8.1].

8.1 Damped atoms and cavities

Perhaps the simplest example we can consider is spontaneous emission from a two-state atom. In this example the picture obtained from the quantum trajectory approach is a picture that has been presented in many guises before. It is the picture of jumps between discrete atomic states inherent in the Einstein rate equations [Eqs. (3.4a) and (3.4b)]. A closely related example is the decay of an optical cavity mode prepared in a Fock state. We will look first at the atomic example and then at the decaying cavity mode.

We consider a single two-state atom (lower state $|1\rangle$ and upper state $|2\rangle$) described by the source master equation (2.26) (with $\bar{n} = 0$). The field radiated by the atom is given in terms of source operators by (2.61). To

make things as simple as possible we will assume that the detector sees the complete 4π solid angle into which the photon is emitted. The source field operator scaled to give photon flux into the detector is then

$$\hat{\mathcal{E}}_s(t) = \sqrt{\gamma}\sigma_-(t - r/c), \tag{8.1}$$

where γ is the Einstein A coefficient and r is the distance from the source to the detector; the overall phase of this field is unimportant since the decomposition of the master equation dynamics we consider is based on intensity. The superoperators $(\mathcal{L} - \mathcal{S})$ and $\mathcal{S}$ that govern the coherent evolution and collapse, respectively, are defined by the relationships

$$\mathcal{S}\bar{\rho}_c = \gamma\sigma_-\bar{\rho}_c\sigma_+, \tag{8.2a}$$

$$(\mathcal{L} - \mathcal{S})\bar{\rho}_c = -i\tfrac{1}{2}\omega_A[\sigma_z, \bar{\rho}_c] - \frac{\gamma}{2}(\sigma_+\sigma_-\bar{\rho}_c + \bar{\rho}_c\sigma_+\sigma_-), \tag{8.2b}$$

where $\bar{\rho}_c$ is the *unnormalized* conditioned density operator – the density operator for the atom conditioned on its past. In this example the conditioned density operator may be written in terms of a pure state wavefunction:

$$\rho_c(t) = |\psi_c(t)\rangle\langle\psi_c(t)|. \tag{8.3}$$

The dynamical evolution of the unnormalized wavefunction $|\bar{\psi}_c(t)\rangle$ is governed by the nonunitary Schrödinger equation

$$\frac{d}{dt}|\bar{\psi}_c\rangle = \frac{1}{i\hbar}H|\bar{\psi}_c\rangle, \tag{8.4a}$$

with the non-Hermitian Hamiltonian

$$H = \tfrac{1}{2}\hbar\omega_A\sigma_z - i\hbar\frac{\gamma}{2}\sigma_+\sigma_-. \tag{8.4b}$$

The evolution generated by (8.4a) is interrupted by collapses

$$|\bar{\psi}_c\rangle \to \hat{C}|\bar{\psi}_c\rangle, \tag{8.5a}$$

with collapse operator

$$\hat{C} = \sqrt{\gamma}\sigma_-. \tag{8.5b}$$

The probability for a collapse to occur in the interval $(t, t + \Delta t]$ is given by

$$\begin{aligned} p_c(t) &= \mathrm{tr}[\mathcal{S}\rho_c(t)]\Delta t \\ &= (\gamma\Delta t)\langle\psi_c(t)|\sigma_+\sigma_-|\psi_c(t)\rangle \\ &= (\gamma\Delta t)\frac{\langle\bar{\psi}_c(t)|\sigma_+\sigma_-|\bar{\psi}_c(t)\rangle}{\langle\bar{\psi}_c(t)|\bar{\psi}_c(t)\rangle} \end{aligned} \tag{8.6}$$

The spontaneous emission example is sufficiently simple that we can actually solve the trajectory equations (8.4a) and (8.5a) analytically. Assume an arbitrary initial condition

$$|\psi_c(0)\rangle \equiv |\psi_c(0)\rangle = c_1(0)|1\rangle + c_2(0)|2\rangle. \tag{8.7}$$

From (8.4a) and (8.4b) we find that the unnormalized amplitudes $\bar{c}_1(t)$ and $\bar{c}_2(t)$ obey the equations

$$\dot{\bar{c}}_1 = \tfrac{1}{2}i\omega_A \bar{c}_1, \tag{8.8a}$$

$$\dot{\bar{c}}_2 = -(\gamma/2 + \tfrac{1}{2}i\omega_A)\bar{c}_2. \tag{8.8b}$$

The solutions are

$$\bar{c}_1(t) = c_1(0)e^{\frac{1}{2}i\omega_A t}. \tag{8.9a}$$

$$\bar{c}_2(t) = c_2(0)e^{-(\gamma/2)t}e^{-\frac{1}{2}i\omega_A t}. \tag{8.9b}$$

The normalized amplitudes are then

$$c_1(t) = \frac{c_1(0)}{\sqrt{|c_1(0)|^2 + |c_2(0)|^2 e^{-\gamma t}}} e^{\frac{1}{2}i\omega_A t}, \tag{8.10a}$$

$$c_2(t) = \frac{c_2(0)e^{-(\gamma/2)t}}{\sqrt{|c_1(0)|^2 + |c_2(0)|^2 e^{-\gamma t}}} e^{-\frac{1}{2}i\omega_A t}. \tag{8.10b}$$

Equations (8.10) provide the solution for the conditioned wavefunction during the coherent evolution that occurs between collapses:

$$|\psi_c(t)\rangle = c_1(t)|1\rangle + c_2(t)|2\rangle$$
$$= \frac{c_1(0)e^{\frac{1}{2}i\omega_A t}|1\rangle + c_2(0)e^{-(\gamma/2)t}e^{-\frac{1}{2}i\omega_A t}|2\rangle}{\sqrt{|c_1(0)|^2 + |c_2(0)|^2 e^{-\gamma t}}}. \tag{8.11}$$

The probability for a collapse during $(t, t+\Delta T]$ is given by

$$p_c(t) = (\gamma \Delta t)\frac{|c_2(0)|^2 e^{-\gamma t}}{|c_1(0)|^2 + |c_2(0)|^2 e^{-\gamma t}}; \tag{8.12}$$

for an initially excited atom ($c_1(0) = 0$) this probability is independent of time. Clearly there is only one collapse in each trajectory since (8.5a) and (8.5b), and (8.9a) and (8.9b) give (after normalizing the states before and after the collapse)

$$|\psi_c(t)\rangle = c_1(t)|1\rangle + c_2(t)|2\rangle \to |1\rangle. \tag{8.13}$$

Once the atom reaches the lower state $|1\rangle$ the nonunitary Schrödinger equation [solutions (8.10)] simply keeps it there forever; obviously, there can be one and only one photon emission from a single undriven atom.

From the solution (8.11) we can get some sense of what the *conditioned* wavefunction means. Equation (8.11) gives the state of the atom conditioned on the fact that it has not yet emitted a photon; it is the state of the atom before it collapses. We find then that if $c_1(0) \neq 0$ this state approaches $|1\rangle$ for times much longer that the lifetime γ^{-1}. What this tells us is that if we have waited many lifetimes without seeing a photon emission, it is very likely that the atom actually began in the lower state $|1\rangle$, from which it

could not emit . Thus, in waiting for a photon that never came we gain the information that the atom must be in the lower state; therefore, the atom reaches the lower state either by a collapse and photon emission [Eq. (8.13)], or by eventually convincing us that it was actually in the lower state all the time.

An atom prepared in the upper state must collapse into the lower state. A sample trajectory for the conditioned wavefunction is defined by a function $c_2(t)$, that starts with $c_2(0) = 1$, and remains constant until some random time at which it switches to the value $c_2(t) = 0$, remaining there forever; similarly, the function $c_1(t)$ starts with $c_1(0) = 0$ and switches up to the value $c_1(t) = 1$, remaining there forever. This is the jump that we all expect as the atom emits its quantum of energy. The time of emission for each quantum trajectory is random; in the computer it is determined by comparing a random number with the collapse probability (8.12) at each step of the stochastic simulation, as described in Sect. (7.5). If a large number of these emissions is simulated and the number of emissions occurring in $(t, t + \Delta t]$ is plotted against t, we recover the exponential decay illustrated in Fig. 8.1. This corresponds to the exponential decay obtained from the emission probability $(\gamma \Delta t)\rho_{22}(t)$, where $\rho_{22}(t) = e^{-\gamma t}$ is the solution to the Einstein rate equations.

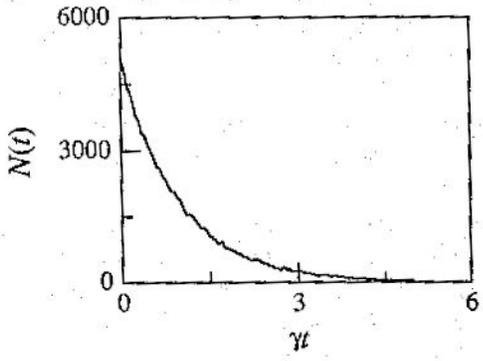

Fig. 8.1. Number of emissions in the interval γt to $\gamma(t + \Delta t)$ versus γt for a simulation of 100,000 spontaneous emission trajectories ($\gamma \Delta t = 0.05$).

The extension of these ideas to the decay of a cavity mode prepared in a Fock state is probably fairly obvious. In this case the operator master equation for the source is (1.47) and the relationship between the radiated field and source operators is given in (1.60). If the detector intercepts the entire cavity output beam, the source field scaled to give photon flux into the detector is

$$\hat{\mathcal{E}}_s(t) = \sqrt{2\kappa}\, a(t - r/c). \tag{8.14}$$

In place of (8.2a) and (8.2b) we have

$$\mathcal{S}\bar{\rho}_c = 2\kappa a \bar{\rho}_c a^\dagger, \tag{8.15a}$$

$$(\mathcal{L} - \mathcal{S})\bar{\rho}_c = -i\omega_C[a^\dagger a \bar{\rho}_c] - \kappa(a^\dagger a \bar{\rho}_c + \bar{\rho}_c a^\dagger a). \tag{8.15b}$$

Once again, the conditioned density operator factorizes as a pure state and satisfies the nonunitary Schrödinger equation (8.4a). The non-Hermitian Hamiltonian is

$$H = \hbar\omega_C a^\dagger a - i\hbar\kappa a^\dagger a. \tag{8.16}$$

The collapse (8.5a) is governed by the collapse operator

$$\hat{C} = \sqrt{2\kappa}\, a, \tag{8.17}$$

and the collapse probability is given by

$$\begin{aligned} p_c(t) &= (2\kappa\Delta t)\mathrm{tr}[\mathcal{S}\rho_c(t)] \\ &= (2\kappa\Delta t)\langle\psi_c(t)|a^\dagger a|\psi_c(t)\rangle \\ &= (2\kappa\Delta t)\frac{\langle\bar{\psi}_c(t)|a^\dagger a|\bar{\psi}_c(t)\rangle}{\langle\bar{\psi}_c(t)|\bar{\psi}_c(t)\rangle}. \end{aligned} \tag{8.18}$$

It is again possible to solve the evolution between collapses analytically. We will not bother with the details. The main point is that the amplitude equations are uncoupled as they are in (8.8a) and (8.8b); consequently, if the cavity mode is in a Fock state, it remains in that Fock state until the next collapse (photon emission) occurs. At that time the effect of the collapse operator (8.17) is to take the Fock state $|n\rangle$ to the Fock state $|n-1\rangle$. Clearly, an initial state $|N\rangle$ will undergo N jumps, at N random times, until the cavity mode reaches the vacuum state, where it will remain forever. A sample trajectory is illustrated in Fig. 8.2(a). On average the dwell time in each Fock state becomes longer as the level of excitation decreases; this is because the collapse probability (8.18) depends on the conditioned mean photon flux $\sqrt{2\kappa}\langle\psi_c(t)|a^\dagger a|\psi_c(t)\rangle$ which decreases as the system descends the random staircase. Figure 8.2(b) shows the evolution of the average intracavity photon number, calculated by averaging 10,000 realizations of the conditioned mean photon number $\langle a^\dagger a\rangle_c \equiv \langle\psi_c(t)|a^\dagger a|\psi_c(t)\rangle$. The ensemble average over trajectories shows the exponential decay given by (3.3).

8.2 Resonance fluorescence

Both of the examples we have just seen are really rather trivial. The quantum trajectories for both are elementary examples of Markoff processes on discrete state spaces. Anyone who is familiar with Markoff processes and a little quantum mechanics could have concocted simulations to produce the quantum trajectories shown in Figs. 8.1 and 8.2. But we have something more than a concoction. We have a well-defined formal procedure for constructing the stochastic process-from an operator master equation. In general the quantum dynamics for a given source will not be as transparent as in the foregoing examples, and the "concoction" approach will not work.

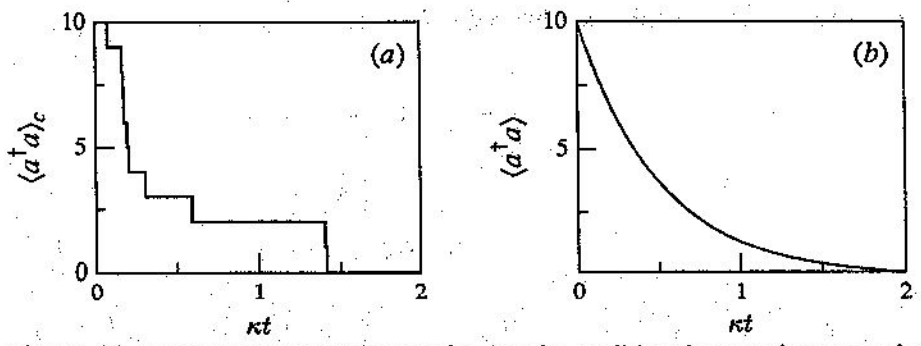

Fig. 8.2. (a) Sample quantum trajectory showing the conditioned mean photon number for a damped cavity mode prepared in the Fock state $|10\rangle$. (b) Average of the conditioned mean photon number for 10,000 trajectories.

The first such nontrivial example we look at is resonance fluorescence. The discussion that follows is an extension of work by Carmichael et al. [8.2].

To model resonance fluorescence the master equation for the atomic source changes from (2.26) to (2.62); we add the dipole interaction with the coherent driving field, proportional to the Rabi frequency Ω. If we keep the assumption that the detector sees all the fluorescence, the source field in photon number units is still (8.1). The collapse of the atomic state is still described by the superoperator relation (8.2a), and (8.2b) changes to

$$(\mathcal{L}-\mathcal{S})\bar{\rho}_c = -i\tfrac{1}{2}\omega_A[\sigma_z,\bar{\rho}_c] - i(\Omega/2)[e^{-i\omega_A t}\sigma_+ + e^{i\omega_A t}\sigma_-,\bar{\rho}_c] - \frac{\gamma}{2}(\sigma_+\sigma_-\bar{\rho}_c + \bar{\rho}_c\sigma_+\sigma_-). \tag{8.19}$$

The rest of the formulation outlined in (8.1)–(8.6) is the same, with the Hamiltonian (8.4b) changed to

$$H = \tfrac{1}{2}\hbar\omega_A\sigma_z + \hbar(\Omega/2)[e^{-i\omega_A t}\sigma_+ + e^{i\omega_A t}\sigma_-] - i\hbar\frac{\gamma}{2}\sigma_+\sigma_-. \tag{8.20}$$

Now from our previous discussion of resonance fluorescence we know that a single fluorescing atom evolves to a stationary state. In conventional language the density operator for the stationary state is defined by (3.64a) and (3.64b). In the quantum trajectory approach we would expect the evolution of the conditioned wavefunction to be governed by a stationary stochastic process. The stochastic process is, in fact, still fairly simple because the collapse relation (8.13) still applies. Thus, after each collapse (photon emission) the atom is in its lower state; this means that the evolution between collapses is always solved from the same initial condition. Unlike the spontaneous emission example, in the presence of the driving field the atom does not remain in the lower state after a collapse; rather, it evolves to a new state $|\psi_c(t)\rangle = c_1(t)|1\rangle + c_2(t)|2\rangle$ with $c_2(t) \neq 0$, where t is now the time since the previous collapse. In this way the atom continuously generates

a nonzero probability for making a further collapse and emitting another photon.

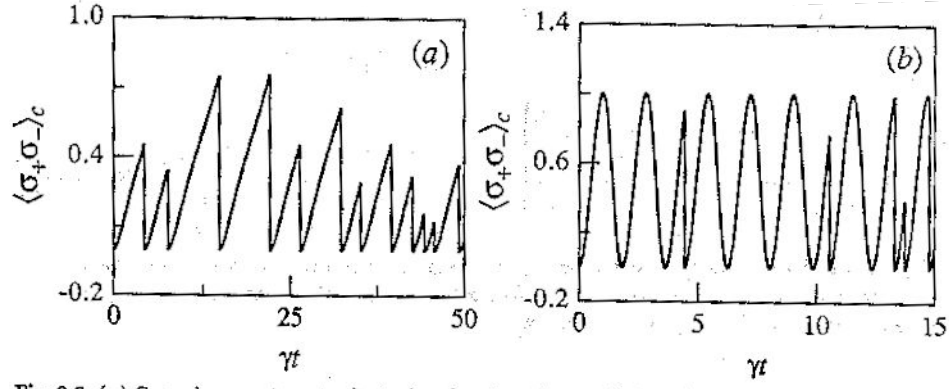

Fig. 8.3. (a) Sample quantum trajectories showing the conditioned upper state probability of an atom undergoing resonance fluorescence. (a) Weak excitation, $\Omega/\gamma = 0.7$; (b) strong excitation, $\Omega/\gamma = 3.5$.

The equations obeyed by the unnormalized amplitudes during the coherent evolution are minor variations of (8.8a) and (8.8b):

$$\dot{\tilde{c}}_1 = \tfrac{1}{2}i\omega_A\tilde{c}_1 + i(\Omega/2)e^{i\omega_A t}\tilde{c}_2, \tag{8.21a}$$

$$\dot{\tilde{c}}_2 = -(\gamma/2 + \tfrac{1}{2}i\omega_A)\tilde{c}_2 + i(\Omega/2)e^{-i\omega_A t}\tilde{c}_1. \tag{8.21b}$$

For an initial state $|\psi_c(0)\rangle = |1\rangle$ the solutions to these equations give the unnormalized amplitudes

$$\tilde{c}_1(t) = e^{-(\gamma/4)t}e^{\frac{1}{2}i\omega_A t}\left[\cosh(\delta t) + \frac{(\gamma/2)}{2\delta}\sinh(\delta t)\right], \tag{8.22a}$$

$$\tilde{c}_2(t) = ie^{-(\gamma/4)t}e^{-\frac{1}{2}i\omega_A t}\frac{\Omega}{2\delta}\sinh(\delta t), \tag{8.22b}$$

where

$$2\delta = \sqrt{(\gamma/2)^2 - \Omega^2}. \tag{8.23}$$

The collapse probability in the time interval $(t, t+\Delta t]$ is then given by

$$p_c(t) = (\gamma\Delta t)|c_2(t)|^2 = (\gamma\Delta t)\frac{|\tilde{c}_2(t)|^2}{|\tilde{c}_1(t)|^2 + |\tilde{c}_2(t)|^2}. \tag{8.24}$$

Figure 8.3 shows two examples of quantum trajectories for resonance fluorescence. The full quantum state could be represented by a stochastic motion on the Bloch sphere; in Fig. 8.3 the upper state probability $|c_2(t)|^2$ is plotted. The vertical jumps return the atom to the lower state at the times of the photon emissions; these are the collapses responsible for photon antibunching in resonance fluorescence (Sect. 3.5). Notice that for

strong excitation [Fig. 8.3(b)] coherent Rabi oscillations occur between the emissions.

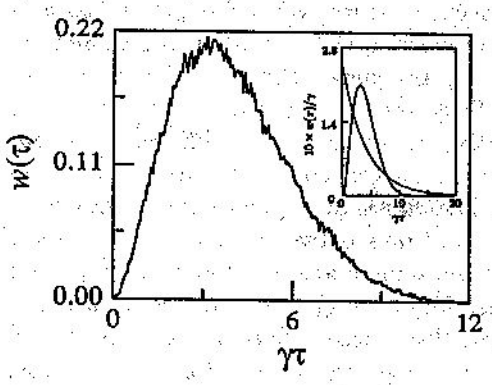

Fig. 8.4. Waiting-time distribution for resonance fluorescence obtained from a histogram of the time intervals between collapses (photon emissions) in the simulation of Fig. 8.3(a). The inset shows the distribution calculated analytically in [8.2].

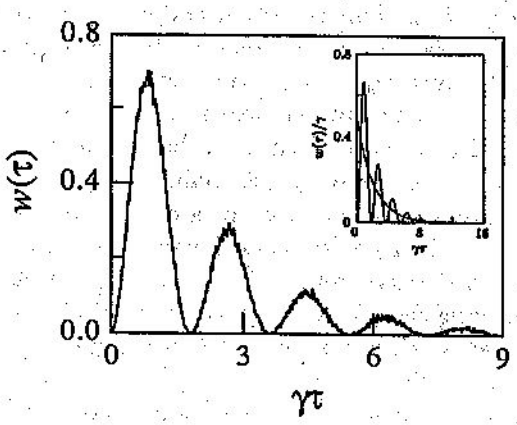

Fig. 8.5. Waiting-time distribution for resonance fluorescence obtained from a histogram of the time intervals between collapses (photon emissions) in the simulation of Fig. 8.3(b). The inset shows the distribution calculated analytically in [8.2].

From simulations like those illustrated in Fig. 8.3 it is possible to carry out photoelectric counting experiments in the computer. We simply count the number of collapses that occur in a counting time T. By repeating the process for many counting intervals we build up a histogram of the number of counting intervals that produce n photoelectron counts. The normalized histogram is the photoelectron counting distribution. We can also obtain waiting-time distributions in an equivalent manner. Figures 8.4 and 8.5 show two examples of waiting-time distributions obtained from quantum trajectories for resonance fluorescence. For comparison the inset shows the waiting-time distribution calculated analytically in [8.2]. The agreement is very good. Of course, the numerical simulations show residual sampling fluctuations, much like those expected in a laboratory experiment.

8.3 Cavity mode driven by thermal light

For an example like resonance fluorescence, where everything needed to simulate the quantum trajectories is contained in (8.22)–(8.24), the numerical simulations are very efficient. However, in general, the numerical work can be increased by a number of factors. First, often it is not possible to solve for the conditioned state $|\psi_c(t)\rangle$ explicitly; then a numerical differential equation solver must do this for us. Second, photon emission sequences in resonance fluorescence are Markoffian. The emission sequences are completely specified by the distribution of waiting times between adjacent emissions. This is because the atom returns to the same state, the lower state $|1\rangle$, on every collapse. After it does this it has forgotten all about where it has been in the past. More generally, each time the source collapses it collapses to a different state. The collapsed state depends on the state before the collapse, which in turn depends on the history of coherent evolution and collapse the source has experienced in the past. In this situation a general solution to the nonunitary Schrödinger equation, for arbitrary initial conditions, is needed.

These complications are likely to be encountered when considering an optical cavity mode as the source. The infinite Fock state basis makes it unlikely that a general solution to the nonunitary Schrödinger equation can be found, and even less likely that a solution exists in a compact form suitable for fast numerics. We now consider a cavity mode driven by thermal light. This is an example where the additional numerical work is required. However, if the intensity of the driving field is not too large, so that the Fock state basis can be truncated at a relatively low level, the numerical requirements are still quite modest.

Thermal excitation adds another complication. Since it is incoherent we are not able to factorize the conditioned density operator as a pure state. Equation (8.15a) holds for describing the collapse. But (8.15b) is replaced by

$$(\mathcal{L}-\mathcal{S})\bar{\rho}_c = -i\omega_C[a^\dagger a\bar{\rho}_c] - \kappa(a^\dagger a\bar{\rho}_c + \bar{\rho}_c a^\dagger a) + 2\kappa\bar{n}(a\bar{\rho}_c a^\dagger + a^\dagger\rho_c a - a^\dagger a\rho_c - \rho_c a^\dagger a); \tag{8.25}$$

the term proportional to $\bar{n}$ does not allow us to use a pure state for describing the evolution between collapses. Nevertheless, the general formalism still holds; it just has to be implemented in density matrix form, with the collapse probability for the interval $(t, t+\Delta t]$ given by

$$p_c(t) = \mathrm{tr}[\mathcal{S}\rho_c(t)]\Delta t = (2\kappa\Delta t)\mathrm{tr}[\rho_c(t)a^\dagger a]. \tag{8.26}$$

Figure 8.6 shows results for $\bar{n} = 1$. The thermal light is turned on at $t = 0$ and the figure shows the transient behavior as the cavity mode approaches a stationary state. Figure 8.6(a) shows a sample quantum trajectory for the conditioned mean photon number $\mathrm{tr}[\rho_c(t)a^\dagger a]$; Fig. 8.6(b) is the average of 10,000 such trajectories and reproduces the exponential filling of the

cavity described by the conventional mean-value equation (3.3). Examples of trajectories for higher intensity light are shown in Fig. (8.7).

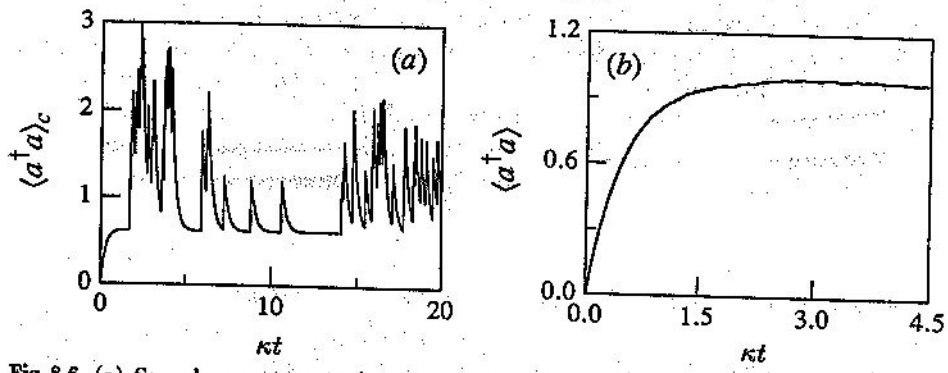

Fig. 8.6. (a) Sample quantum trajectory showing the conditioned mean photon number for a cavity driven by thermal light. The thermal light turns on at $t = 0$ and injects a photon flux $2\kappa\bar{n} = 2\kappa$ ($\bar{n} = 1$). The Fock state basis is truncated at 20 photons. (b) Ensemble average of 10,000 such trajectories.

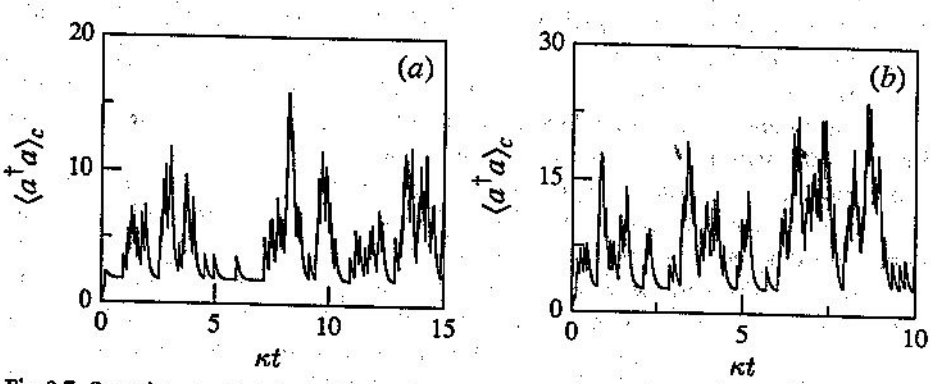

Fig. 8.7. Sample quantum trajectories showing the conditioned mean photon number for a cavity driven by thermal light. (a) The thermal light turns on at $t = 0$ and injects a photon flux $2\kappa\bar{n} = 10\kappa$ ($\bar{n} = 5$). The Fock state basis is truncated at 50 photons. (b) The thermal light turns on at $t = 0$ and injects a photon flux $2\kappa\bar{n} = 20\kappa$ ($\bar{n} = 10$). The Fock state basis is truncated at 80 photons.

These trajectories show a surprising feature that tells us a little more about the nature of the conditioned quantum state. The sudden jumps in the conditioned mean photon number occur when the state collapses as a photon is emitted from the cavity. But the jumps are upwards, not downwards as in Fig. 8.2. How can the emission of a photon make the number of photons in the cavity increase? The explanation is that the conditioned mean photon number is the mean of $a^\dagger a$ with respect to a state that is conditioned on

everything that has taken place along the trajectory in the past. Every twist of this trajectory adds information to the memory. The conditioned mean photon number propagates information; it is not an actual photon number *out there* in the cavity. For a thermal state the observation of one collapse, one photon emitted, means another is very likely, at twice the average rate, immediately following the first. Thus, the photon bunching of thermal light (Sect. 3.4) is built into the conditioned state as *upwards jumps* in the conditioned mean photon number, which gives upwards jumps in the collapse probability [Eq. (8.26)] immediately following each collapse.

8.4 The degenerate parametric oscillator

Lecture 6 was devoted to the homodyne detection of squeezed light. In the next lecture we will see how the quantum trajectory approach can be used to treat homodyne detection. But first, let us look at squeezed light by direct photoelectric detection. The source master equation is based on the master equation (2.63) for the degenerate parametric oscillator. However, we will not take this master equation directly as it is written. We are interested in below threshold operation, where the quantum-classical correspondence led us to the Fokker-Planck equations (4.72) and (4.73). In these equations the coupling between fluctuations in the pump mode and the subharmonic mode has disappeared; the pump field simply enters the Fokker-Planck equation for the subharmonic mode through the parameter λ. We can build this simplification into the master equation directly. Essentially, we assume that the density operator ρ factorizes into a product of density operators for the two cavity modes. We then write a master equation for each. The density operator for the pump mode satisfies the master equation for a cavity driven by the coherent field $\bar{\mathcal{E}}_i$ – the second, fourth, and sixth terms on the right-hand side of (2.63); the master equation for the subharmonic mode is obtained from the first, third, and fifth terms on the right-hand side of (2.63), with the coherent state amplitude of the pump substituted for the operator b:

$$\dot{\rho} = -i\omega_C[a^\dagger a, \rho] + (\kappa\lambda/2)[a^{\dagger 2}e^{-i2\omega_C t} - a^2 e^{i2\omega_C t}, \rho] + \kappa(2a\rho a^\dagger - a^\dagger a\rho - \rho a^\dagger a). \tag{8.27}$$

Here λ is the pump parameter defined below (4.64).

Now the superoperator governing the collapse is defined by (8.15a) and the coherent evolution between collapses is governed by

$$(\mathcal{L} - \mathcal{S})\bar{\rho}_c = -i\omega_C[a^\dagger a, \bar{\rho}_c] + (\kappa\lambda/2)[a^{\dagger 2}e^{-i2\omega_C t} - a^2 e^{i2\omega_C t}, \bar{\rho}_c] - \kappa(a^\dagger a\bar{\rho}_c + \bar{\rho}_c a^\dagger a). \tag{8.28}$$

It is again possible to factorize $\bar{\rho}_c$ as a pure state and use the nonunitary Schrödinger equation (8.4a). The non-Hermitian Hamiltonian is

$$H = \hbar\omega_C a^\dagger a + i\hbar(\kappa\lambda/2)(a^{\dagger 2}e^{-i2\omega_C t} - a^2 e^{i2\omega_C t}) - i\hbar\kappa a^\dagger a. \tag{8.29}$$

The collapse probability for the interval $(t, t+\Delta t]$ is calculated from (8.18).

A sample quantum trajectory for the conditioned mean photon number in the subharmonic mode is shown in Fig. 8.8(a). Figure 8.8(b) is the average of 10,000 such trajectories and shows the build-up of the mean photon number in the cavity after the pump is turned on at $t = 0$. Note how, once again, the collapse can cause an *upwards* jump in the conditioned mean photon number. In this example some of the jumps are upwards and some are downward. The reason for this is that photons are created in pairs inside the cavity. When the first photon of a pair is emitted from the cavity the conditioned mean photon number, and hence the collapse probability (8.18), makes an upwards jump; this ensures that the second photon will be emitted within a short time [$\sim (2\kappa)^{-1}$] after the first. After the second photon has been emitted the collapse decreases the conditioned mean photon number, which in a few cavity lifetimes returns to its steady-state value.

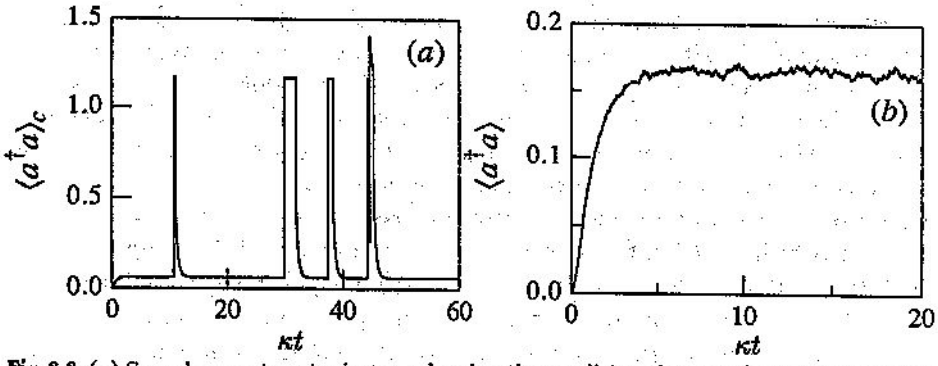

Fig. 8.8. (a) Sample quantum trajectory showing the conditioned mean photon number for a degenerate parametric oscillator operated 50% below threshold ($\lambda = 0.5$). The pump light is turned on a $t = 0$. The Fock state basis is truncated at 10 photons. (b) Ensemble average of 10,000 such trajectories.

The pairing of photon emissions leads to an imbalance between even and odd numbers of photoelectron counts in the photoelectron counting distribution. We have already mentioned this in Sect. 6.5. Figure 8.9 shows a photoelectron counting distribution obtained by counting the collapses (photon emissions) for many quantum trajectories of the sort illustrated in Fig. 8.8(a). The even-odd oscillations are large. The inset shows the distribution obtained by Wolinsky and Carmichael [8.3] for the same parameters, using a related but quite different method. This photoelectron counting distribution also agrees with the results of Vyas and Singh [8.4] which are obtained analytically.

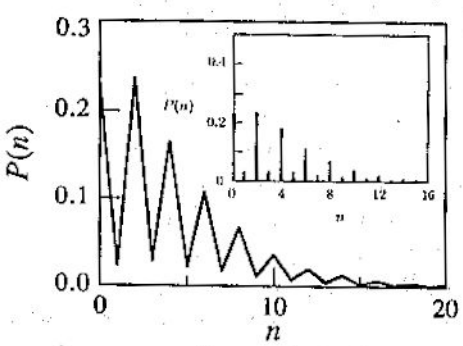

Fig. 8.9. Photoelectron counting distribution for the output of a degenerate parametric oscillator obtained by counting collapses (photon emissions) in the simulation of Fig. 8.8(a). The inset shows the photoelectron counting distribution obtained be other methods [8.3, 8.4].

8.5 Complementary unravellings

In all of the examples we have looked at during this lecture the decomposition of the source master equation dynamics has been based on the direct photoelectric detection of the radiated light. From the stochastic quantum trajectories obtained in this way we can calculate quantities such as average intensities, waiting-time distributions, and photoelectron counting distributions – quantities that are measured by direct photoelectric detection. From the concrete visualization that the quantum trajectory approach allows, we also gain some understanding of the physical processes going on in the source. The decomposition we have used is not, however, unique; it is tailored for direct photoelectric detection. We cannot use the quantum trajectories obtained from this decomposition to calculate everything we might be interested in (at least not in a simple way), nor do these trajectories help us understand every nook and cranny of the quantum dynamics.

In Sect. 7.4 we referred to the decomposition of the source master equation to give quantum trajectories as an *unravelling of the master equation for the source*. The quantum dynamics contained in the master equation are unravelled to give us a picture of what is going on in a visible form. The pictures we have presented so far reveal what is going on when we focus our attention on emitted photons (direct photoelectric detection). Other unravellings of the master equation will give us different pictures, suited to help us understand different aspects of the physics. The complete picture is the complement of all the separate pictures, and by the very nature of quantum mechanics no single picture can substitute for them all. In a way, our difficulty in understanding the full quantum mechanical evolution lies in the fact that the one master equation carries the many pictures forward in parallel. We gain a lot by separating the pictures out.

In the next lecture we will see how to use the quantum trajectory approach to analyze the homodyne detection of squeezed light. By modeling homodyne detection we arrive at a quite different unravelling of the master equation (8.27). In fact, we obtain an infinity of unravellings, one for each choice of the local oscillator phase. As an introduction, Fig. 8.10 shows a

sample trajectory for the conditioned mean photon number for two different choices of the local oscillator phase. These correspond to a measurement of the unsqueezed quadrature X and the squeezed quadrature Y of the fluctuating field amplitude. These trajectories look nothing like the trajectory shown in Fig. 8.8(a); they are even qualitatively different from each other, one showing much larger fluctuations than the other. However, all three of these trajectories are equivalent in the mean. They are complementary unravellings of the quantum average $\mathrm{tr}[\rho(t)a^\dagger a]$ (note that it is not the conditioned density operator here); the time average of all three produces exactly the same number.

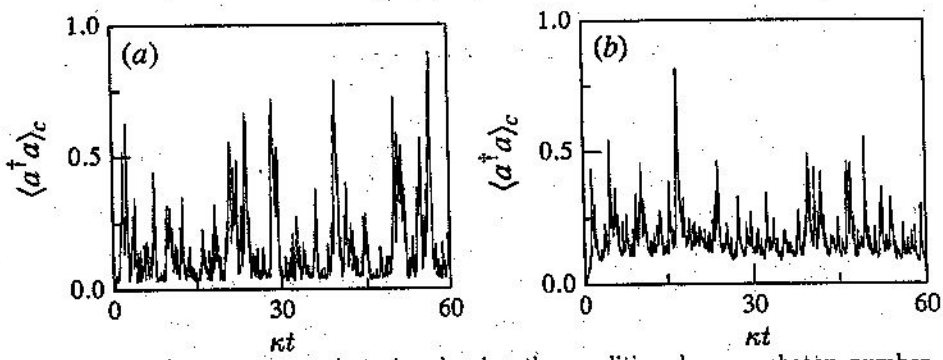

Fig. 8.10. Sample quantum trajectories showing the conditioned mean photon number obtained from the unravelling of the degenerate parametric oscillator master equation described in Sec. 9.2. The parametric oscillator is operated 10% below threshold ($\lambda = 0.9$). (a) The unravelling is based on a measurement of the X-quadrature variance; (b) the unravelling is based on a measurement of the Y-quadrature variance.

References

[8.1] H. J. Carmichael and L. Tian, "Quantum Measurement Theory of Photoelectric Detection," in *OSA Annual Meeting Technical Digest 1990*, Vol. 15 of the OSA Technical Digest Series, Optical Society of America: Washington, D. C., 1990, p. 3.

[8.2] H. J. Carmichael, S. Singh, R. Vyas, and P. R. Rice, *Phys. Rev.* A **39**, 1200 (1989).

[8.3] M. Wolinsky and H. J. Carmichael, "Photoelectron Counting Statistics for the Degenerate Parametric Oscillator," in *Coherence and Quantum Optics VI*, ed. by J. H. Eberly, L. Mandel, and E. Wolf, Plenum: New York, 1989, pp. 1239ff.

[8.4] R. Vyas and S. Singh, *Opt. Lett.* **14**, 1110 (1989); *Phys. Rev.* A **40**, 5147 (1989).